Wave Reflection: More Than A "Round Trip"

Rashid Ghorbani Afkhami[1], Sarah J. Johnson[1]

[1] School of Electrical Engineering & Computing, The University of Newcastle, Australia

Author for correspondence

Mr. Rashid Ghorbani Afkhami, School of Electrical Engineering & Computing, The University of Newcastle, Australia

Email: rashid.ghorbaniafkhami@uon.edu.au

Abstract

Reflected pressure waves are key to the understanding of vascular aging, a prominent factor in major cardiovascular events. Several different metrics have been proposed to index the effect of wave reflection on the pressure waveform and thereby serve as an indicator of vascular aging. The extent to which these indices are influenced by factors other than vascular health remains a matter of concern. In this paper, we will first derive a mathematical model for the reflection time (T_{refl}), and the augmentation index (AI), assuming a general extended model of the arterial system. Then, we test our model against values reported in the literature. Finally, we discuss insights from the model to common observations in the literature such as age-related "shift" in the reflection site, the variation of AI with heart rate, and the flattening of T_{refl} in older participants. Our results indicate that although both T_{refl} and AI are affected by aging, the load properties are important factors to consider. Especially for T_{refl}, the delay caused at the load site can account for more than 50% of its value. The comparison between model outputs and reported values confirms the validity of the model. The proposed model describes how vascular parameters affect the reflection time and the augmentation index.

Keywords: aging, arteries, wave reflection, augmentation index, blood pressure.

1 Introduction

Vascular aging is a prominent factor in major cardiovascular events including stroke, heart failure and coronary artery disease [1]. Vascular health is studied through pulsatile arterial hemodynamics and several key indicators of vascular aging have been identified in pulsatile pressure readings such as the pulse wave velocity (PWV), reflection time (T_{refl}), and augmentation index (AI) [1, 2].

In particular, reflected waves are frequently studied to infer cardiovascular properties [2]. Reflected waves occur when forward traveling pressure waves hit an effective reflection site (which is a superimposition of several sites in practice) and are reflected back towards their source (in this case the heart). In elastic arteries appropriately timed reflected waves help maintain pressure during diastole, however, they can have an ill-effect as age progresses and PWV increases. With increased PWV, which more than doubles in the aorta between the ages of 17 and 70 [3], reflected waves advance into the systole and add to the systolic pressure [4]. This increases peak systolic, end diastolic pressure and mean arterial pressure [5] and contributes to stress on the vessels [2].

The concept of reflection time, pulse transit time or pulse return time was defined on the central pressure waveform as the timing of the inflection point [6]. When a forward traveling pressure waveform from the left ventricle combines with the reflected wave, it leaves a visible curvature called the inflection point. Similarly, on more distal pressure waveforms, the pulse transit time is defined as the time difference between the first (systolic) and second (reflected) peaks [7]. Both definitions aim to capture the same phenomenon, the latter one measures peak to peak difference of the forward and reflected waves whereas the former method measures the foot to foot time differences. Here, we will refer to this timing as the reflection time, T_{refl}. T_{refl} is commonly formulated as

$$T_{\text{refl}} = \frac{2d_0}{\text{PWV}} \tag{1}$$

where d_0 is the distance from the measurement site to the reflection site, multiplied by two to account for a round trip. The equation simply calculates the travel time by dividing distance to travel speed. This equation is commonly used to assess vascular compliance or to estimate d_0 [5, 6, 8, 9, 10, 11, 12, 13, 14, 15, 16]. It should be noted that (1) holds only when a resistive load is assumed, i.e., a real load (in a mathematical sense) impedance [6, 16, 17]. However, a pure resistive load can not sufficiently model distal arteries [17]. In elderly populations (>65 years) T_{refl} reaches a plateau state whereas PWV still increases and the first conclusion from (1) is increased d_0, the apparent distal shift of the reflection site after this age [5, 10] which contradicts with the accepted opinion [18]. The debate of changes in d_0 has been the topic of several publications [5, 6, 10, 17]. In this paper will examine the controversy of moving reflection site and other observations for the reported T_{refl} and AI values by understanding these indices from a mathematical viewpoint using a model of the vascular tree.

A number of models have already been developed to study the vascular system. Two-element Windkessels were the first generation in the form of an RC circuit [2]. Later, a third element was added in series to model the characteristic impedance of the arterial tube, the model is called the three-element Windkessel (WK3) [19, 20, 21]. The Windkessel models, although popular and efficient for parameter estimation due to their simplicity, were unable to reflect the finite pulse wave velocity and thus the wave propagation phenomenon and the presence of the reflected waves in the arterial system. Thereby, transmission line (TL) equations and models were adopted to understand the changes in flow and pressure at the same pace as they advance in the arteries [20, 22].

In this paper, we assume a WK3 at the load and use the transmission line theory to formulate T_{refl} and AI in terms of the model parameters. Then, we use the reported values in the literature for each parameter and compare measured T_{refl} and AI values to the model outputs. After validating our models for T_{refl} and AI, we use them to gain insights into commonly observed measurements.

2 Method

In this section we will first briefly review the TL theory then define T_{refl} and AI in terms of the model parameters and finally we will show how the model fits to different data reported in the literature.

2.1 Model Derivation

The approach is based on a uniform transmission line model of the vascular system used in the literature [20, 22], see Fig. 1. The heart is located at $x = -d$ with blood pressure and flow of P_{H} and Q_{H}, respectively. Z_0 is the characteristic impedance of the transmission line and the reflection site has the blood pressure and flow of P_{L} and Q_{L}, respectively terminated by a three-element Windkessel with its third element, Z_0, matching the characteristic impedance of the line. R and C are the resistance and the compliance, respectively, resembling the properties of the vascular system beyond the reflection site. It should be mentioned that a tapered model [23] can be used instead of a uniform model, however, given a fixed measurement distance the two models can be shown to be equivalent given an appropriate optimization of the parameters [24]. Note that the TL model accounts only for the pulsatile components of the pressure and flow.

The pressure as a function of time and distance can be decomposed into forward and backward traveling elements, i.e.,

$$P(x) = P_{\mathrm{f}}(x) + P_{\mathrm{b}}(x). \tag{2}$$

In which $P_{\mathrm{f}}(x)$, $P_{\mathrm{b}}(x)$ are the forward and backward (reflected) traveling waveforms. These waveforms are in the form of

$$P_{\mathrm{f}}(x) = p_{\mathrm{f}} e^{-\gamma x}, \quad P_{\mathrm{b}}(x) = p_{\mathrm{b}} e^{\gamma x}, \tag{3}$$

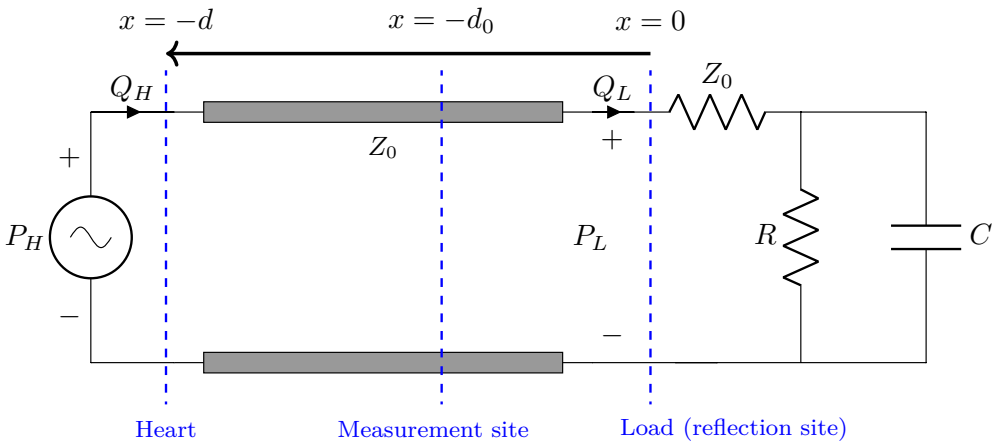

Figure 1: Transmission line model

where p_f and p_b have complex quantities in general and are calculated using the boundary conditions. γ and x are the propagation constant and distance from the load, respectively. Note that (2) and (3) are phasor domain solutions to the transmission line equations assuming steady state sinusoidal pressure and flow input waveforms. For a lossless case, the time domain solution will be

$$p(x,t) = |p_{\mathrm{f}}| \cos(\omega t - \beta x + \phi_{\mathrm{f}}) + |p_{\mathrm{b}}| \cos(\omega t + \beta x + \phi_{\mathrm{b}}), \tag{4}$$

where $|p_{\mathrm{f}}|\, e^{j\phi_{\mathrm{f}}}$ and $|p_{\mathrm{b}}|\, e^{j\phi_{\mathrm{b}}}$ are the amplitude and phase of p_{f} and p_{b} in (3), respectively and β, which is equal to the imaginary part of γ, is called the phase constant. The reflection coefficient is defined as the ratio of the reflected pressure wave to the incident pressure wave, i.e.,

$$\Gamma(x) = \frac{P_{\mathrm{b}}(x)}{P_{\mathrm{f}}(x)} = \frac{p_{\mathrm{b}} e^{j\beta x}}{p_{\mathrm{f}} e^{-j\beta x}} = \frac{p_{\mathrm{b}}}{p_{\mathrm{f}}} e^{j2\beta x}. \tag{5}$$

2.1.1 Reflection Time

In order to formulate the reflection time using the transmission line theory, let Φ be the phase difference between the forward and the reflected waves at $x = -d_0$ along the line, which will be equal to the absolute value of the phase of the reflection coefficient at the same

location, $\theta_\Gamma(x = -d_0)$, i.e,

$$\Phi = |\theta_\Gamma(-d_0)| = |\theta_\Gamma(0) - 2\beta d_0| \,. \tag{6}$$

To calculate $\theta_\Gamma(0)$, first we should quantify the reflection coefficient at the load, $x = 0$. We have

$$\Gamma(0) = \frac{Z_L - Z_0}{Z_L + Z_0}, \tag{7}$$

where $Z_L = P(0)/Q(0)$, see Fig. 1. Also, with a WK3 at the load, see Fig.1, we have

$$Z_L = Z_0 + \frac{R}{1 + j\omega RC}, \tag{8}$$

inserting into (7) gives

$$\Gamma(0) = \frac{R}{R + 2Z_0 + 2j\omega Z_0 RC}, \tag{9}$$

with its phase equal to

$$\theta_\Gamma(0) = -\tan^{-1} \frac{2\omega Z_0 RC}{R + 2Z_0}. \tag{10}$$

Using the first order Taylor series expansion on (10) and inserting into (6) we get

$$\Phi \approx \frac{2\omega Z_0 RC}{R + 2Z_0} + 2\beta d_0. \tag{11}$$

The phase constant, β, is related to the pulse wave velocity (or propagation velocity) as $\beta = \omega/\text{PWV}$. Also, note that we are interested in measuring the time difference between the forward and the reflected wave, T_{refl}, which is the phase difference, Φ, divided by the angular velocity, ω. Inserting these into (11) we have

$$T_{\text{refl}} \approx \underbrace{\frac{2Z_0 RC}{R + 2Z_0}}_{\Delta t_{\text{load}}} + \underbrace{\frac{2d_0}{\text{PWV}}}_{\Delta t_{\text{line}}}, \tag{12}$$

which breaks the travel time of the reflected wave into two elements. Δt_{line} is the delay caused by the line itself which is influenced by the speed on the line and the length of the line. Δt_{load} is the delay at the load, in particular forced by the capacitive properties of the load. Thus, the wave reflection is more than a simple "round trip", there is a delay in between.

It should be noted that the reflection site (Fig. 1) in the proposed model is a symbolic reflection location which represents reflections from various reflection and re-reflection sites [25]. Therefore, d_0, the distance between the measurement and the reflection sites, does not indicate a specific location on the arterial system with reference to the measurement site and in fact it can have a value which is larger than what one would expect based on vascular structure. The reason is the existence of re-reflection sites which are closer to the heart than the point of the measurement and reflect back the already reflected waves [25]. These waves with much larger d_0 also add up to the measured pressure contributing to the reflected pressure waveform.

2.1.2 Augmentation Index

The augmentation index or AI is defined as

$$\text{AI} = \frac{P_{\text{refl}} - P_{\text{dia}}}{P_{\text{sys}} - P_{\text{dia}}}, \tag{13}$$

in which P_{refl}, P_{dia} and P_{sys} are peak reflection, end-diastolic and peak systolic blood pressures, respectively [26]. This definition is commonly used to report AI for the arteries distal to the heart with two distinctive peaks visible in the waveform. For proximal arteries where reflected and the incident waves often overlap, another definition is used.

$$\text{AI}^* = \frac{P_{\text{refl}} - P_{\text{sys}}}{P_{\text{max}} - P_{\text{dia}}}, \tag{14}$$

where $P_{\max} = \max\{P_{\text{refl}}, P_{\text{sys}}\}$ [8, 14, 27, 28, 29]. AI^* can be expressed in terms of AI as

$$\text{AI}^* = \begin{cases} 1 - 1/\text{AI} & P_{\text{refl}} > P_{\text{sys}} \,(\text{i.e., } P_{\max} = P_{\text{refl}}) \\ 0 & P_{\text{refl}} = P_{\text{sys}} \\ \text{AI} - 1 & P_{\text{refl}} < P_{\text{sys}} \,(\text{i.e., } P_{\max} = P_{\text{sys}}) \end{cases} \tag{15}$$

It is known that the reflected waves have negligible contribution during the period between end-diastole and peak-systole because of the lossy line properties of the arterial tree. Therefore, with the absence of the reflected wave we can assume

$$P_{\text{sys}} \approx \text{MAP} + |p_{\text{f}}|\,, \tag{16}$$

where MAP is the mean arterial pressure. MAP in practice is closer to the end-diastole than the peak systole, because of the differences in systolic and diastolic durations. For instance the end diastole, MAP and peak systole are reported in [30] as 77.5, 93.0 and 124.1 mmHg, respectively. Which shows that systolic peak difference to MAP is twice as great as the end-diastolic peak difference from MAP. Here, for the practicality of the formulation we use the same concept, i.e.,

$$P_{\text{dia}} \approx \text{MAP} - \frac{1}{2}\,|p_{\text{f}}|\,. \tag{17}$$

Now, to quantify the reflected peak value, we should be mindful of the phase difference between the forward and backward traveling waves. Based on the approach taken in Section 2.1.1, when the reflected wave reaches its maximum value, the incident wave drops its amplitude by the factor of $\cos\Phi$ or $\cos(\omega T_{\text{refl}})$. This means

$$P_{\text{refl}} \approx \text{MAP} + |p_{\text{f}}|\cos(\omega T_{\text{refl}}) + |p_{\text{b}}|\,. \tag{18}$$

In which the second term is the amplitude of the forward traveling wave when the reflected peak happens and the third term is the maximum value of the backward traveling wave at

the same time. Inserting (16), (17) and (18) into (13) we get

$$\mathrm{AI} \approx \frac{2}{3}\left(\cos\left(\omega T_{\mathrm{refl}}\right) + |\Gamma(0)| + \frac{1}{2}\right), \tag{19}$$

as our formula for AI. AI^* can be calculated from (19) using (15). Also, note that in this section we are not assuming sinusoidal waveforms except to define $\mathrm{T_{refl}}$ in (18).

2.2 Model

In this study we compare the values reported in the literature with values derived from our models. It is important to note that we do not "fit" our model to the data. All model parameters are published values from the literature. Among the input variables to the model the parameters R and C are load properties which will be far from the heart and compliant vessels regardless of the measurement site and therefore location-independent values can be selected for these parameters. However, characteristic impedance, Z_0 and PWV are both line properties which can change as the measured location is moved distal from the heart. Here, we will ignore the PWV increase from aorta to radial artery (the farthest artery we will examine) as this is reported to be small [31] and this will not affect the model results. Yet, we will try to match Z_0 to its realistic values depending on the artery of interest.

2.3 Case I

In a large-scaled study [32], 2026 healthy middle-aged subjects are divided into four half-decade age ranges with mean group ages of 37.5, 43, 48 and 53.5 years. The pressure waveform is measured from the left common carotid artery using applanation tonometry (flow was measured from the aorta using ultrasound). The mean and standard deviation (SD) values for heart rate (HR), characteristic impedance (we used the frequency-domain method results) and systemic vascular resistance, R, for men and women are reported for each age group [32], see Table 1.

Parameter		Mean value of the age group	
HR	M	$[61.1 \pm 9.1, 61.2 \pm 9.2, 63.1 \pm 10.3, 61.8 \pm 9.9]$	bpm
	F	$[65.3 \pm 9.0, 65.8 \pm 8.8, 65.2 \pm 8.5, 65.4 \pm 8.1]$	
Z_0	M	$[155, 136, 135, 134]$	$10^{-4}\text{KPa} \cdot \text{cm}^{-3} \cdot \text{s}$
	F	$[155, 150, 145, 145]$	
R	M	$[1654, 1690, 1688, 1713]$	$10^{-4}\text{KPa} \cdot \text{cm}^{-3} \cdot \text{s}$
	F	$[1650, 1677, 1722, 1804]$	
C	M	$[4.785, 5.010, 4.875, 4.740]$	$10^{-1}\text{KPa}^{-1} \cdot \text{cm}^3$
	F	$[2.781, 2.726, 2.642, 2.531]$	

Table 1: HR, Z_0 and R values as reported in [32] for men (M) and women (F). Scaled C values are based on [32] and [33].

Although total arterial compliance is already reported in [32], we are interested in load compliance values which are much smaller than when the proximal compliant vessels are involved in the calculations. Therefore, we used mean compliance values of the arteries distal to the heart (referred to as oscillatory compliance in [33]) measured by invasive methods in [33] (4.852 and 2.670 in the units of $10^{-1}\text{KPa}^{-1} \cdot \text{cm}^3$ for men and women, respectively) to downscale the values reported in [32], see Table 1. That is, the compliance values (calculated from the pulse pressure method) reported for each age group for men were scaled so that the total mean value would be the same as the one reported in [33], and the same was done for the values reported for women. We have set $d_0 = 40$ cm for men and $d_0 = 35$ cm for women which covers an approximate distance from the arch of aorta to the end of internal carotid artery.

The final carotid T_{refl} model for this case was calculated as per our formula, (12), with load compliance values derived from [33] and [32], d_0 of 40 cm and 35 cm, respectively for men and women, and PWV, Z_0 and R as reported in [32] for gender and age group. The values in Table 1 were also used to calculate the model estimated T_{refl} in (1).

Next, to estimate the augmentation index the values of the reflection coefficient at the load site, i.e., $|\Gamma(0)| = |p_{\text{b}}| \,/\, |p_{\text{f}}|$, are needed. These values are calculated in [32] as the amplitude of the reflection coefficient at the heart rate. Using the measured $|\Gamma(0)|$ and estimated T_{refl} values into (19) and then (15) gives us the model estimated AI^* values.

2.4 Case II

For this case we used the data of 266 healthy participants (age range of 18-78 years and mean ± SD of 37.9 ± 18.9 years) reported in [7]. Radial arterial pressure was measured using applanation tonometry and the time interval between the first and the second systolic peaks was calculated as T_{refl}. None of the model inputs are reported in [7] and therefore, for this case we used values reported in other literature as follows. Values of C are measured with invasive methods in [33] for 115 healthy volunteers. Although a linear relationship between C and age is derived in [33], non-linear changes are noticeable in the scatter plot and thus we digitized the data to fit an exponential function as

$$C = 12.39 \times \exp\left(-0.0277 \times \text{Age}\right) + g_{\text{c}}. \tag{20}$$

Where g_{c} is a gender correction parameter, set to +0.77 and -0.70 respectively for men and women to satisfy $C_{\text{men}}(\text{Age} = 40) = 4.85$ and $C_{\text{women}}(\text{Age} = 47) = 2.67$ reported in [33] for mean age in each group (same units as of Table 1 used here). To model R in healthy volunteers aged less than 50 years, we have used the linear increase reported in [33], first line of (21). However, for ages more than 50 years we have proposed an exponential relationship, second line of (21). That is

$$R = \begin{cases} 8.1 \times \text{Age} + 926.9 + g_{\text{r}} & \text{Age} \leq 50 \\ 333.4 \times \exp(0.0277 \times \text{Age}) + g_{\text{r}} & \text{Age} > 50 \end{cases}. \tag{21}$$

This is based on a comprehensive blood pressure study of 2036 participants, stating that the estimation of the vascular resistance using mean blood pressure underestimates the actual resistance value at the ages above 50 to 60 years [34]. The exponential factor is set to the similar rate as of the observed exponential rate in C, i.e., 0.0277, and the amplitude of 333.4 is to avoid discontinuity at the Age = 50. The gender correction factor, g_{r}, is set to -32 and +105 respectively for men and women to satisfy $R_{\text{men}}(\text{Age} = 40) = 1219$ and

$R_{\text{women}}(\text{Age} = 47) = 1413$ [33] (same units as of Table 1 used here).

Pulse wave velocity has the form of

$$\text{PWV} = 10 \times \text{Age} + 300 \quad \left(\text{cm} \cdot \text{s}^{-1}\right) \tag{22}$$

as reported in [35] measured from the ascending aorta and matches the results in [36]. Finally, we estimated the characteristic impedance as $Z_0 = 1.185$ KPa $\cdot$ cm^{-3} $\cdot$ s with a WK3 fit to the synthetic data provided in [37]. Based on the results reported in [32], Z_0 either does not change with age or the changes are negligible thus we used a constant $Z_0 = 1.185$ for all ages. We also set $d_0 = 20$ cm and $d_0 = 16$ cm, respectively for men and women corresponding to the length of radial artery (mean value of 18 cm has been reported for the radial artery [38]).

Putting mentioned values for each parameter into (12) and (1), we obtain estimated radial T_{refl} values for our model and the existing model, respectively.

2.5 Case III

A radial augmentation index is reported in [26] for 632 healthy subjects, where AI is defined as in (13). Age-independent heart rate values are reported as 70.6 ± 11.0 and 71.5 ± 9.5 (mean $\pm$ SD beats per minute) for men and women, respectively [26]. For this case, all other inputs were selected as described in Section 2.4. First, T_{refl} was calculated as per (12) and then, using (9), $|\Gamma(0)|$ was calculated. Substituting into (19) results the modeled AI for the radial artery.

2.6 Case IV

Changes of aortic T_{refl} with PWV in 73 outpatients (age range 17-95 years, mean age 51.8 years) have been reported in [39], where pressure waveforms are recorded with non-invasive methods from the carotid artery and were assumed to be similar to the pressure values in the ascending aorta and central arteries. Reported values were not separated by gender and

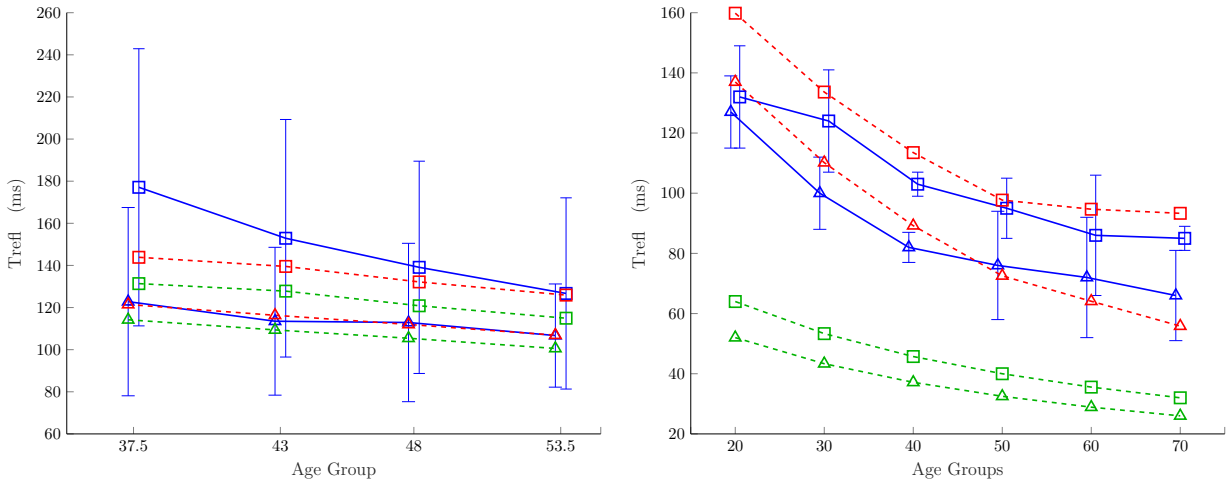

(a) (b)

Figure 2: T_{refl} in carotid (a) case I and radial (b) case II for men (square) and women (triangle). Measured (blue) data is from the literature [7, 32] and estimated values are from the new proposed model (red) and the existing model (green). Values are in the form of mean ± SD.

so we used (20) and (21) to obtain gender-independent estimates of C and R with $g_c = 0$ and $g_r = 0$, respectively. We set $d_0 = 40$ cm and $Z_0 = 0.136$ KPa $\cdot$ cm^{-3} $\cdot$ s, estimated for the carotid artery using a WK3 fit on the synthetic data of [37]. Results are gender-independent carotid reflection times for the new and the existing model using (12) and (1), respectively calculated using the same age range of [39] i.e., 17-95 years.

3 Results

The formulas derived from the model were validated numerically against the numbers reported in the literature. For cases I-III the results are shown in Fig. 2 and Fig. 3 and for case IV the results are in Fig. 4. Note that case I reports AI* whereas case III reports AI and that AI* values reported in [32] are in the form of mean and standard errors of mean which have been converted into mean ± SD. Error bars for estimated AI in case III are only due to heart rate variability and no other variation has been taken into account. The results show high similarity between modeled T_{refl} and AI and measured values and a high level

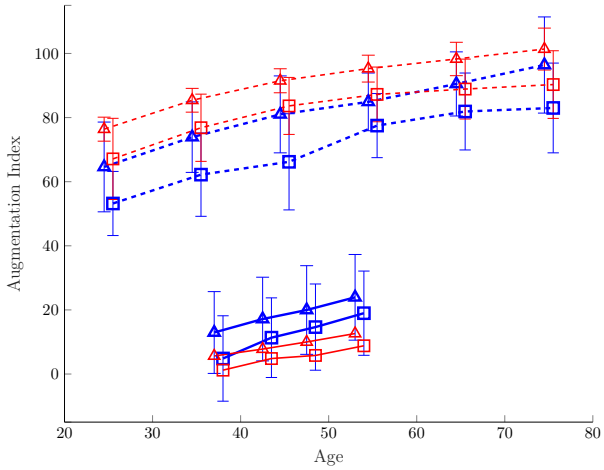

Figure 3: Measured (blue) and estimated (red) augmentation index for men (square) and women (triangle) in carotid (solid line, case I) [32] and radial (dashed line, case III) [26] arteries. Values are in the form of mean ± SD.

of improvement for the estimation of the reflected wave compared to the existing model, especially in the radial artery.

Carotid AI* for young adults is reported to be negative which then turns positive as age progresses [40, 41]. Based on our model $P_{\text{refl}}/P_{\text{sys}} = \cos\omega T_{\text{refl}} + |\Gamma(0)|$ gives estimated $P_{\text{refl}}/P_{\text{sys}}$ values ranging from 1.02 to 1.14 and from 1.09 to 1.22 for men and women, respectively for case I. With a linear regression on model outputs we speculate that at the ages of 34.0 and 24.9 years respectively for men and women we will have $P_{\text{refl}} = P_{\text{sys}}$ and thus AI*=0 for this case, see Fig. 3. Carotid AI* zero crossing has been reported at the ages of 31.7 years for total of 38 male and 18 female participants in [40] and 23.7 years for 74 male and 60 female participants in [41]. This, is another prediction from the model which is confirmed in the literature.

4 Discussion

In this paper we have formulated a mathematical model for T_{refl} including dependencies on both line and load properties. Through several case studies we have compared our models for T_{refl} and AI against published measured data, and have shown that we can closely match

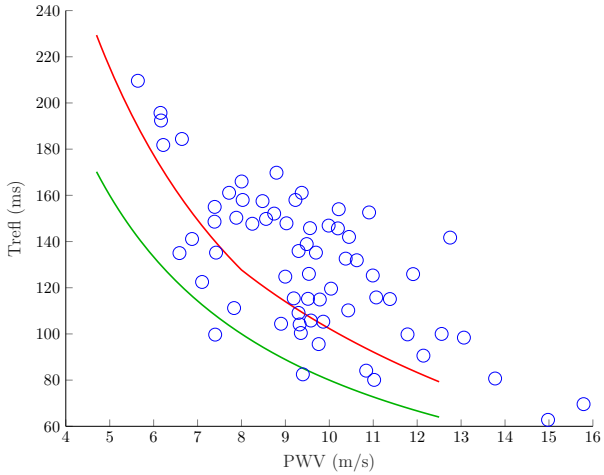

Figure 4: Estimated carotid T_{refl} against PWV using the proposed model (red) and the existing model (green) compared with measured values from [39] (case IV) in blue.

the observed data. We can thus apply these models to give insights into several observed phenomena which we discuss in this section.

Several studies have reported a strong correlation between T_{refl} and age [5, 7, 11]. Based on our model we can see that the load site delay of the reflection time, Δt_{load}, is primarily influenced by the compliance of the load, as the resistance properties, R and Z_0, are found in both numerator and denominator of the model in (12) and so cancel out to some extent. In addition, PWV itself is a function of the line compliance (the compliance of the arteries between the measurement site and the reflection site, commonly used as an index of vascular compliance [42]) and combined with the influence of load compliance (the WK3 compliance at the load) makes T_{refl} a strong index of overall vascular compliance with only weak effects from vascular resistance. It is well known that compliance decreases with age; therefore, based on our model the correlation of the reflection time with age is due to strong dependence on changes in compliance and PWV with age.

It is reported in the literature that T_{refl} does not decrease linearly with age in elder populations and in fact it almost flattens after the age of 65 years [5, 6, 17]. The flattening effect is reflected in our model, see Fig. 2, through three main components. First, the nonlinear relationship of the load compliance with age shown in (20). Based on the data

reported in [33], measured load compliance does not decrease as sharply with age in older populations. Second, vascular resistance, R, increases exponentially after the age of 50 years, see (21), which contributes to an increase in Δt_{load} and thus T_{refl}. This ultimately stops Δt_{load} from dropping which weakens the T_{refl} dependency on age and compliance in older populations. The third component is the influence of characteristic impedance making the effect highly dependent on the sight of measurement. Based on our estimates from the data in [37] the value of Z_0 increases almost ten-fold moving from carotid to radial artery. The small Z_0 values in proximal arteries heighten the flattening effect in T_{refl}. As an example, with all three elements in effect, based on the model for case IV, carotid T_{refl} drops 37 ms from 10 to 20 years and only 9 ms from 80 to 90 years. Thus, based on our model the flattening of the reflection time is due to exponential changes in compliance and vascular resistance with age. Also, the effect is more noticeable in proximal arteries due to the decreased impedance in large vessels.

It has been reported that the effective reflection site moves distally after the age of 65 years [5, 10], although this view is challenged in several studies [6, 17]. Our model is able to explain this phenomenon by shedding light on the delay that the reflected wave sees at the load site, Δt_{load}. Note that the Δt_{load} portion of T_{refl} is usually ignored in the analysis [5, 6, 8, 9, 10, 14, 15, 17], despite the hints given in [23] and [17]. Based on our model Δt_{load} can account for up to 25% (case IV) and 62% (case II) of T_{refl} in carotid and radial arteries, respectively. Δt_{load} gets relatively larger compared to Δt_{line} when moving distal from the heart for two main reasons; the decrease of d_0 and the increase of Z_0. Fig. 2 and Fig. 4 have examples of radial and carotid T_{refl} acquired from (1) for case II and IV, respectively. Thus, the results reported in [5, 10] using (1) should be treated with care and our model in (12) can be used for more accurate interpretations of the location of the reflection site.

It is reported in the literature that reflection time does not show a notable change with heart rate, only 10 ms drop in radial T_{refl} is reported for heart rate ranging from 60 to 80 beats per minute for the data in case II [7]. Our model confirms the independence of heart

rate and T_{refl} as heart rate does not affect the calculated T_{refl} in (12).

The augmentation index has been shown to have negative correlations with T_{refl} [43] and heart rate [44] and positive correlation with age [10, 26, 40]. Our model also shows these effects and describes AI, see (19), as a function of T_{refl}, heart rate and reflection coefficient. Even in extreme cases, $\max(T_{refl}) < 0.25$ s and $\max(f_{HR}) < 0.5$ Hz (f_{HR} being heart rate frequency) and therefore, $0 < \omega T_{refl} < \pi/2$ suggesting that the cosine function is monotonically decreasing and AI will always increase with decreased T_{refl} or decreased heart rate, explaining the negative correlation. Thus our model suggests that the positive correlation of AI with age is due to decreased T_{refl} with aging and the negative correlation between AI and heart rate is due to the presence of the cosine function.

A flattening effect is repeatedly reported for the augmentation index [10, 13, 28]. It has been observed that AI/AI* flattens after the age of 55 years [28] and can even decline thereafter [10]. Although no decline in AI/AI* was observed in the proposed model, the flattening is noticeable in model outputs as age progresses with only 1.3% and 2.8% increase in radial AI (case III) between the ages of 65 and 75 years for men and women, respectively. The AI/AI* flattening is due to the flattening of the reflection time, since the other influencing element of the augmentation index is the reflection coefficient which increases, only slightly, with age [32]. Thus, our model suggests the observed flattening in AI/AI* is due to age related increase in vascular resistance and more importantly, a slowing of the decrease in compliance with age.

4.1 Study Limitations

The proposed model contains a series of theoretical assumptions that form simplified relationships between desired vascular aging indices and comprehensible model elements, and is subject to practical limitations which hinder the model validation.

Theoretical Assumptions: The Taylor series expansion in (11) holds only for small values of arctangent argument, x, i.e., $|x| < 1$. However, based on published values [26] we

have $\max(x) = 0.50$ radian, making this assumption reasonable for our model.

By assuming a lossless transmission line we are not accounting for reductions in pressure as the pressure wave propagates along the vessel, where in reality the reflected waves will lose power traveling towards the heart. Thus, we may overestimate $|\Gamma(0)|$ in estimation of the augmentation index. Nonetheless, the results are less affected in distal arteries, as $|\Gamma(0)|$ is not a dominant factor in the calculation of AI. First, because Z_0 increases and second, the reflection time is shorter and thus $\cos \omega T_{\text{refl}}$ is becoming the dominant factor in AI.

Practical Limitations: In practice, the calculation of the peak-to-peak time difference between forward and backward waves is difficult, especially in proximal arteries where forward and backward waves do not leave separate peaks. Therefore, various methods have been developed for calculation of the return of the reflected waves. Reflection time is calculated in [32] (case I) using the 4^{th} derivative method [45], referred to as the "shoulder time", T_{sho} in [11] whereas [39] (case IV) uses the time of the occurrence of the inflection point, T_{inf}, as described in [11]. Wave separation analysis can also be used to calculate the time difference of the forward and backward waves using the zero-crossing point of each waveform, called $T_{\text{f-b}}$ in [11]. The theoretical approach in this paper uses the peaks of the forward and backward waves to calculate T_{refl}, which is different to the definition of $T_{\text{f-b}}$ as each wave shows different rise time from zero-crossing to the peak. However, the modeled T_{refl} best matches the definitions of T_{sho} and T_{inf} in [11].

The study was limited by the reported measurements of model input parameters. Especially, age related increase of systemic vascular resistance was reported only in a small number of papers. Although a linear increase of R with age is reported in [46] and [33], it is suggested that R values are underestimated in older subjects [34]. More investigation is required to accurately model changes in R with age.

5 Conclusion

In this paper, we formulated mathematical models for two widely used pressure waveform indices, T_{refl} and AI using a transmission line model ended with a three-element Windkessel load. Derived formulas were successfully applied to data reported in the literature. The results confirmed the dependency of both indices on vascular aging indicators: compliance, PWV and systemic vascular resistance. The model was able to explain the flattening of T_{refl} repeatedly reported in the literature, as well as the moving of the reflection site which is a subject of controversy in the literature. We also showed that a larger portion of T_{refl} might be due to the delay caused at the load by the compliance at the reflection point. Overall, our results suggest that T_{refl} is strongly influenced by vascular compliance and represents a useful index of vascular compliance in populations younger than 65. In older populations T_{refl} remains influenced by vascular compliance but its effects are reduced due to an exponential increase in vascular resistance in those older than 50 which has an opposite effect on T_{refl}. AI is itself inversely dependent on T_{refl} so shows a similar flattening with age, however it is also strongly affected by heart rate, which will influence AI values independently of vascular compliance.

References

[1] H.-Y. Lee and B.-H. Oh, "Aging and arterial stiffness," *Circulation Journal*, vol. 74, no. 11, pp. 2257–2262, 2010.

[2] W. W. Nicholas and M. F. O'Rourke, *McDonald's Blood Flow In Arteries: Theoretical, Experimental and Clinical Principles*, 5th ed. Hodder Arnold, 2005.

[3] M. F. O'Rourke and R. P. Kelly, "Wave reflection in the systemic circulation and its implications in ventricular function," *Journal of Hypertension*, vol. 11, no. 4, pp. 327–337, 1993.

[4] A. J. Baksi, T. A. Treibel, J. E. Davies, N. Hadjiloizou, R. A. Foale, K. H. Parker, D. P. Francis, J. Mayet, and A. D. Hughes, "A meta-analysis of the mechanism of blood pressure change with aging," *Journal of the American College of Cardiology*, vol. 54, no. 22, pp. 2087–2092, 2009.

[5] J. Sugawara, K. Hayashi, and H. Tanaka, "Distal shift of arterial pressure wave reflection sites with aging," *Hypertension*, vol. 56, no. 5, pp. 920–925, 2010.

[6] T. S. Phan, J. K. Li, P. Segers, M. Reddy-Koppula, S. R. Akers, S. T. Kuna, T. Gislason, A. I. Pack, and J. A. Chirinos, "Aging is associated with an earlier arrival of reflected waves without a distal shift in reflection sites," *Journal of American Heart Association*, vol. 5, no. 9, 2016.

[7] Y. Zhang, Y. Zheng, Z. Ma, and S. Y., "Radial pulse transit time is an index of arterial stiffness," *Hypertension Research*, vol. 34, no. 7, pp. 884–887, 2011.

[8] J. P. Murgo, N. Westerhof, J. P. Giolma, and S. A. Altobelli, "Aortic input impedance in normal man: relationship to pressure wave forms." *Circulation*, vol. 62, no. 1, pp. 105–116, 1980.

[9] R. D. Latham, N. Westerhof, P. Sipkema, B. J. Rubal, P. Reuderink, and J. P. Murgo, "Regional wave travel and reflections along the human aorta: a study with six simultaneous micromanometric pressures." *Circulation*, vol. 72, no. 6, pp. 1257–1269, 1985.

[10] G. F. Mitchell, H. Parise, E. J. Benjamin, M. G. Larson, M. J. Keyes, J. A. Vita, R. S. Vasan, and D. Levy, "Changes in arterial stiffness and wave reflection with advancing age in healthy men and women," *Hypertension*, vol. 43, no. 6, pp. 1239–1245, 2004.

[11] P. Segers, E. R. Rietzschel, M. L. D. Buyzere, D. D. Bacquer, L. M. V. Bortel, G. D. Backer, T. C. Gillebert, and P. R. Verdonck, "Assessment of pressure wave reflection: getting the timing right!" *Physiological Measurement*, vol. 28, no. 9, pp. 1045–1056, aug 2007.

[12] A. Qasem and A. Avolio, "Determination of aortic pulse wave velocity from waveform decomposition of the central aortic pressure pulse," *Hypertension*, vol. 51, no. 2, pp. 188–195, 2008.

[13] C. M. McEniery, Yasmin, I. R. Hall, A. Qasem, I. B. Wilkinson, and J. R. Cockcroft, "Normal vascular aging: Differential effects on wave reflection and aortic pulse wave velocity: The anglo-cardiff collaborative trial (acct)," *Journal of the American College of Cardiology*, vol. 46, no. 9, pp. 1753 – 1760, 2005.

[14] W. W. Nicholas and B. M. Singh, "Augmentation index as a measure of peripheral vascular disease state," *Current Opinion in Cardiology*, vol. 17, no. 5, pp. 543–551, 9 2002.

[15] J. P. Lekakis, N. A. Zakopoulos, A. D. Protogerou, T. G. Papaioannou, V. T. Kotsis, V. C. Pitiriga, M. D. Tsitsirikos, K. S. Stamatelopoulos, C. M. Papamichael, and M. E. Mavrikakis, "Arterial stiffness assessed by pulse wave analysis in essential hypertension: relation to 24-h blood pressure profile," *International Journal of Cardiology*, vol. 102, no. 3, pp. 391 – 395, 2005.

[16] B. E. Westerhof and N. Westerhof, "Magnitude and return time of the reflected wave: the effects of large artery stiffness and aortic geometry," *Journal of Hypertension*, vol. 30, no. 5, pp. 932–939, 2012.

[17] B. E. Westerhof, J. P. van den Wijngaard, J. P. Murgo, and N. Westerhof, "Location of a reflection site is elusive," *Hypertension*, vol. 52, no. 3, pp. 478–483, 2008.

[18] M. F. O'Rourke and W. W. Nichols, "Changes in wave reflection with advancing age in normal subjects," *Hypertension*, vol. 44, no. 6, pp. E10–E11, 2004.

[19] W. K. Laskey, H. G. Parker, V. A. Ferrari, W. G. Kussmaul, and A. Noordergraaf, "Estimation of total systemic arterial compliance in humans," *Journal of Applied Physiology*, vol. 69, no. 1, pp. 112–119, 1990.

[20] R. Burattini and K. B. Campbell, "Effective distributed compliance of the canine descending aorta estimated by modified t-tube model." *The American journal of physiology*, vol. 264 6 Pt 2, pp. H1977–87, 1993.

[21] N. Westerhof, J.-W. Lankhaar, and B. E. Westerhof, "The arterial windkessel," *Medical and Biological Engineering and Computing*, vol. 47, no. 2, pp. 131–141, 2008.

[22] G. Zhang, J.-O. Hahn, and R. Mukkamala, "Tube-load model parameter estimation for monitoring arterial hemodynamics," *Frontiers in Physiology*, vol. 2, no. 72, pp. 1–18, 2011.

[23] B. E. Westerhof and N. Westerhof, "Uniform tube models with single reflection site do not explain aortic wave travel and pressure wave shape," *Physiological Measurement*, vol. 39, no. 12, p. 124006, dec 2018.

[24] A. Mousavi, A. Tivay, B. Finegan, M. S. McMurtry, R. Mukkamala, and J.-O. Hahn, "Tapered vs. uniform tube-load modeling of blood pressure wave propagation in human aorta," *Frontiers in Physiology*, vol. 10, p. 974, 2019.

[25] J. E. Davies, J. Alastruey, D. P. Francis, N. Hadjiloizou, Z. I. Whinnett, C. H. Manisty, J. Aguado-Sierra, K. Willson, R. A. Foale, I. S. Malik, A. D. Hughes, K. H. Parker, and J. Mayet, "Attenuation of wave reflection by wave entrapment creates a horizon effect in the human aorta," *Hypertension*, vol. 60, no. 3, pp. 778–785, 2012.

[26] K. Kohara, Y. Tabara, A. Oshiumi, Y. Miyawaki, T. Kobayashi, and T. Miki, "Radial augmentation index: A useful and easily obtainable parameter for vascular aging," *American Journal of Hypertension*, vol. 18, no. S1, pp. 11S–14S, 01 2005.

[27] R. Kelly, C. Hayward, A. Avolio, and M. O'Rourke, "Noninvasive determination of age-related changes in the human arterial pulse." *Circulation*, vol. 80, no. 6, pp. 1652–1659, 1989.

[28] F. Fantin, A. Mattocks, C. J. Bulpitt, W. Banya, and C. Rajkumar, "Is augmentation index a good measure of vascular stiffness in the elderly?" *Age and Ageing*, vol. 36, no. 1, pp. 43–48, 11 2006.

[29] I. Wilkinson, S. Fuchs, I. Jansen, J. Spratt, G. Murray, J. Cockcroft, and D. Webb, "Reproducibility of pulse wave velocity and augmentation index measured by pulse wave analysis," *Journal of Hypertension*, vol. 16, no. 12, pp. 2079–2084, 1998.

[30] H. D. Sesso, M. J. Stampfer, B. Rosner, C. H. Hennekens, J. M. Gaziano, J. E. Manson, and R. J. Glynn, "Systolic and diastolic blood pressure, pulse pressure, and mean arterial pressure as predictors of cardiovascular disease risk in men," *Hypertension*, vol. 36, no. 5, pp. 801–807, 2000.

[31] N. Bjarnegård, C. Bengtsson, J. Brodszki, G. Sturfelt, O. Nived, and T. Länne, "Increased aortic pulse wave velocity in middle aged women with systemic lupus erythematosus," *Lupus*, vol. 15, no. 10, pp. 644–650, 2006.

[32] P. Segers, E. R. Rietzschel, M. L. D. Buyzere, S. J. Vermeersch, D. D. Bacquer, L. M. V. Bortel, G. D. Backer, T. C. Gillebert, and P. R. Verdonck, "Noninvasive (input) impedance, pulse wave velocity, and

wave reflection in healthy middle-aged men and women," *Hypertension*, vol. 49, no. 6, pp. 1248–1255, 2007.

[33] G. E. McVeigh, C. W. Bratteli, D. J. Morgan, C. M. Alinder, S. P. Glasser, S. M. Finkelstein, and J. N. Cohn, "Age-related abnormalities in arterial compliance identified by pressure pulse contour analysis," *Hypertension*, vol. 33, no. 6, pp. 1392–1398, 1999.

[34] S. S. Franklin, W. Gustin, N. D. Wong, M. G. Larson, M. A. Weber, W. B. Kannel, and D. Levy, "Hemodynamic patterns of age-related changes in blood pressure," *Circulation*, vol. 96, no. 1, pp. 308–315, 1997.

[35] E. R. Gozna, A. E. Marble, A. Shaw, and J. G. Holland, "Age-related changes in the mechanics of the aorta and pulmonary artery of man." *Journal of Applied Physiology*, vol. 36, no. 4, pp. 407–411, 1974.

[36] A. P. Avolio, S. G. Chen, R. P. Wang, C. L. Zhang, M. F. Li, and M. F. O'Rourke, "Effects of aging on changing arterial compliance and left ventricular load in a northern chinese urban community." *Circulation*, vol. 68, no. 1, pp. 50–58, 1983.

[37] M. Willemet and J. Alastruey, "Arterial pressure and flow wave analysis using time-domain 1-d hemodynamics," *Annals of Biomedical Engineering*, vol. 43, no. 1, pp. 190–206, Jan 2015.

[38] H. Shima, K. Ohno, K. ich Michi, K. Egawa, and R. Takiguchi, "An anatomical study on the forearm vascular system," *Journal of Cranio-Maxillofacial Surgery*, vol. 24, no. 5, pp. 293 – 299, 1996.

[39] G. London, A. Guerin, B. Pannier, S. Marchais, A. Benetos, and M. Safar, "Increased systolic pressure in chronic uremia. role of arterial wave reflections." *Hypertension*, vol. 20, no. 1, pp. 10–19, 1992.

[40] K. Hirata, T. Yaginuma, M. F. O'Rourke, and M. Kawakami, "Age-related changes in carotid artery flow and pressure pulses," *Stroke*, vol. 37, no. 10, pp. 2552–2556, 2006.

[41] J. Nurnberger, A. Keflioglu-Scheiber, A. M. Opazo Saez, R. R. Wenzel, T. Philipp, and R. F. Schafers, "Augmentation index is associated with cardiovascular risk," *Journal of Hypertension*, vol. 20, no. 12, pp. 2407–2414, 2002.

[42] G. M. London, B. Pannier, and M. E. Safar, "Arterial stiffness gradient, systemic reflection coefficient, and pulsatile pressure wave transmission in essential hypertension," *Hypertension*, vol. 74, no. 6, pp. 1366–1372, 2019.

[43] I. B. Wilkinson, H. MacCallum, P. C. Hupperetz, C. J. van Thoor, J. R. Cockcroft, and D. J. Webb, "Changes in the derived central pressure waveform and pulse pressure in response to angiotensin ii and noradrenaline in man," *The Journal of Physiology*, vol. 530, no. 3, pp. 541–550, 2001.

[44] I. B. Wilkinson, H. MacCallum, L. Flint, J. R. Cockcroft, D. E. Newby, and D. J. Webb, "The influence of heart rate on augmentation index and central arterial pressure in humans," *The Journal of Physiology*, vol. 525, no. 1, pp. 263–270, 2000.

[45] K. Takazawa, N. Tanaka, K. Takeda, F. Kurosu, and C. Ibukiyama, "Underestimation of vasodilator effects of nitroglycerin by upper limb blood pressure," *Hypertension*, vol. 26, no. 3, pp. 520–523, 1995.

[46] W. W. Nichols, M. F. O'Rourke, A. P. Avolio, T. Yaginuma, J. P. Murgo, C. J. Pepine, and C. Conti, "Effects of age on ventricular-vascular coupling," *American Journal of Cardiology*, vol. 55, pp. 1179–1184, 1985.